J Therm Anal Calorim (2011) 103:1095–1103
DOI 10.1007/s10973-010-1197-7

Determination of heat capacities and thermodynamic properties of two structurally unrelated but isotypic calcium and manganese(II) 2,6-naphthalene dicarboxylate-based MOFs

Chun-Hong Jiang · Li-Fang Song · Cheng-Li Jiao · Jian Zhang · Li-Xian Sun · Fen Xu · Huan-Zhi Zhang · Qing-Yang Xu · Zelimir Gabelica

Received: 1 September 2010 / Accepted: 15 November 2010 / Published online: 14 December 2010

Abstract Two metal-organic frameworks, Ca(2,6-NDC)(DMF) (**1**) and $Mn_3(2,6\text{-NDC})_3(DMF)_4$ (**2**) (where 2,6-NDC = 2,6-naphthalene dicarboxylate and DMF = *N,N′*-dimethylformamide) have been solvothermally synthesized under optimized conditions and characterized by X-ray powder diffraction, elemental analysis, FT-IR spectroscopy, and TG analysis. The thermal decomposition characteristics were investigated under air atmosphere from 300 to 1,170 K (for **1**) and from 300 to 971 K (for **2**). The molar heat capacities were measured from 198 to 548 K (for **1**) and from 198 to 448 K (for **2**) by temperature modulated differential scanning calorimetry (TMDSC) for the first time. The fundamental thermodynamic parameters such as entropy and enthalpy variations with temperature were calculated based on the experimentally determined molar heat capacities.

Keywords Ca-MOF · Mn^{II}-MOF · Molar heat capacity · TG · Temperature-modulated DSC

C.-H. Jiang · L.-F. Song · C.-L. Jiao · J. Zhang · L.-X. Sun (✉) · H.-Z. Zhang · Q.-Y. Xu
Materials and Thermochemistry Laboratory, Dalian Institute of Chemical Physics, Chinese Academy of Sciences, 457 Zhongshan Road, Dalian 116023, People's Republic of China
e-mail: lxsun@dicp.ac.cn

C.-H. Jiang · L.-F. Song · C.-L. Jiao
Graduate School of the Chinese Academy of Sciences, Beijing 100049, People's Republic of China

F. Xu (✉)
Faculty of Chemistry and Chemical Engineering, Liaoning Normal University, Dalian 116029, People's Republic of China
e-mail: xufen@lnnu.edu.cn

Z. Gabelica
Université de Haute Alsace, ENSCMu, Lab. LPI-GSEC, 3, Rue A. Werner, 68094 Mulhouse Cedex, France

Introduction

Metal-organic frameworks (MOFs) are molecular architectures comprising metal ion nodes bridged by organic ligands, which have attracted much interest recently due to their potential interest for gas storage [1–5], gas separation [6–10], as catalytic active phases [11–15], and as luminescent materials [16–18]. Among the numerous synthetic routes leading to MOF materials, most of them involve the use of metal carboxylates as organic ligands that readily interact with various metal ions through their negatively charged ends. The 2,6-naphthalene dicarboxylate ligand (2,6-NDC) has been used as an efficient linker for constructing frameworks of coordination polymers [19], due to its significant rigidity and marked stability [20]. In particular, among compounds prepared in the presence of diethylformamide (DEF) used as solvent and co-ligand, $Zn_4O(2,6\text{-NDC})_3(DEF)_6$ was shown to exhibit a large surface area and thereby an important gas sorption capacity, while $Mg_3(2,6\text{-NDC})_3(DEF)_4$ framework showed a high H_2 adsorption enthalpy and a selective uptake of H_2 and O_2 over N_2 and CO [21–23]. Similar (2,6-NDC)-based microporous compounds involving Mg [20] and Li [24] have been reported. The Mg compound, involving a permanent porosity with a large Langmuir surface area and specific pore volume, showed a significant hydrogen storage capacity. Among the Li-based lightweight MOF materials another compound synthesized in the presence of 1,3–BDC and dimethylformamide (DMF), $Li_2(1,3\text{–BDC})(DMF)_{0.5}$, recently also proved highly sensitive to water and methanol [26].

Molar heat capacities of such materials at different temperatures are basic data in chemistry and engineering, from which many other thermodynamic parameters such as

enthalpy and entropy can be calculated. These parameters are important for both theoretical and practical purposes. In particular, while the molar C_p values could be helpful to check the purity of the various phases or possibly the occurrence of some phase transition at a certain temperature, such as detected in the case of cobalt 5,10,15,20-tertrakis (4-metoxyphenyl)-21*H*-23H-porphirine [27], both the enthalpy and entropy values at a given temperature, that are closely related to the fundamental physical and chemical properties of a compound, could be potentially useful to explain/predict the sorptive properties (different gas uptakes) of porous MOF materials under various conditions.

Temperature modulated differential scanning calorimetry (TMDSC) is one of the easiest and very accurate methods for determining heat capacities. This method has been extensively developed for a straightforward determination of heat capacities for various MOF-type materials, isothermally and non-isothermally [27–32].

In this study, we have selected two MOF compounds, namely Ca(2,6-NDC)(DMF) (**1**) and Mn_3(2,6-NDC)$_3$-(DMF)$_4$ (**2**), constructed from 2,6-NDC and DMF and involving two different divalent cations, The composition of their monocationic unit cells suggests that they can have an isotypic relationship but their real structure described in [33] and [34], respectively, proved significantly different in terms of both metal and ligand coordination, thereby resulting in different assemblies and different sterical hindrances. More specifically in **1**, the building blocks consist in polymeric metal-carboxylate chain motives. The chain of metal cations is bridged to carboxylate moieties and DMF molecules. Ca^{2+} cations are 6-, 7-, and 8-coordinated to oxygens, yielding Ca–O distances of 2.35, 2.39, and 2.45 Å, respectively [33]. In **2**, the linear trimeric clusters are linked via 6 carboxylate groups to the NDC ligands to form a 3D network. The central metal atom is octahedrally coordinated by 6 carboxylate oxygens while the 2 peripheral Mn ions link 4 carboxylate and 2 DMF oxygens, achieving a distorted octahedral geometry. Carboxylate groups adopt both bidentate and tridentate coordination to bridge Mn ions.

Compounds **1** and **2** were prepared by slightly modifying the literature recipes [33, 34]. Their nature (structure) and purity were checked by chemical analysis, FTIR (spectra not shown) and powder XRD. Their thermal decomposition patterns were investigated by TG so as to confirm (for **2**) or to determine (for **1**) their initial stability (temperature domain in which reliable thermodynamic data could be derived), and their further decomposition scheme. Their molar heat capacities were measured by TMDSC within their stability domains, namely from 198 to 548 K for **1** and from 198 to 448 K for **2**. The thermodynamic parameters, namely enthalpy and entropy, were then calculated from the experimental molar $C_{p,m}$ values.

Experimental

All reagents were commercially available and were of analytical grade unless stated elsewhere.

Sample preparation

Ca(2,6-NDC)(DMF), **1**. $Ca(NO_3)_2{\cdot}4H_2O$ (0.236 g, 1 mmol) and 2,6-NDC (0.216 g, 1 mmol) were dissolved in 24 ml *N,N′*-dimethylformamide. The homogenized mixture was sealed in a 50 mL Teflon-lined stainless steel autoclave and heated at 120 °C for 3 days, then left to cool to room temperature. The resulting yellow blocky, almost isometric crystals were isolated by filtration, washed thoroughly with DMF and finally dried in vacuum at 60 °C overnight. Yield: 87.62%, based on Ca.

Mn_3(2,6-NDC)$_3$(DMF)$_4$, **2**. We have followed the "conventional solvothermal procedure" proposed in [34], except that we used Mn chloride instead of nitrate and a final admixture less concentrated in DMF. $MnCl_2{\cdot}4H_2O$ (0.148 g, 0.75 mmol) and 2,6-NDC (0.165 g, 0.75 mmol) were dissolved in 20 ml *N,N′*-dimethylformamide. The mixture was sealed in a 50 mL Teflon-lined stainless steel autoclave and heated at 110 °C for 24 h, then cooled naturally to room temperature. The resulting yellow needle-shaped crystals were isolated by filtration, washed thoroughly with DMF, and finally dried in vacuum at 60 °C overnight. Yield and crystal size are similar as reported [34].

Characterization

Elemental analysis was carried on PE-2400 II Series CHNS/O analyzer. FT-IR spectra were recorded on a Nicolet 380 FT-IR spectrometer using KBr pellet in the wavelength range of 4,000–400 cm^{-1}. Powder X-ray diffraction patterns (PXRD) were recorded on a X'Pert PRO X-ray diffractometer using CuKα radiation (40 kV, 40 mA). The PXRD patterns of the as-synthesized compounds **1** and **2** and their simulated patterns are shown in Fig. 1.

Elemental analysis (%) for **1** calculated: C 55.04, H 4.02; found: C 54.68, H 4.87; and for **2** calculated: C 52.43, H 4.22; found: C 53.26, H 4.03.

FT-IR for **1**: 3,423 cm^{-1}, ν(O–H); 3,070–2,942 cm^{-1}, ν_s(C–H); 1,648–1,362 cm^{-1}, ν(aromatic C=C); 798–673 cm^{-1}, ν_s(aromatic C–H); For **2**: 3,440 cm^{-1}, ν(O–H); 2,992–2,905 cm^{-1}, ν_s(C–H); 1,669–1,399 cm^{-1}, ν(aromatic C=C); 798–673 cm^{-1}, ν_s(aromatic C–H).

Thermal analysis

Thermogravimetric analysis (TG) was carried out on Cahn Thermax 500 from 321 to 1,170 K (**1**) and from 304 to

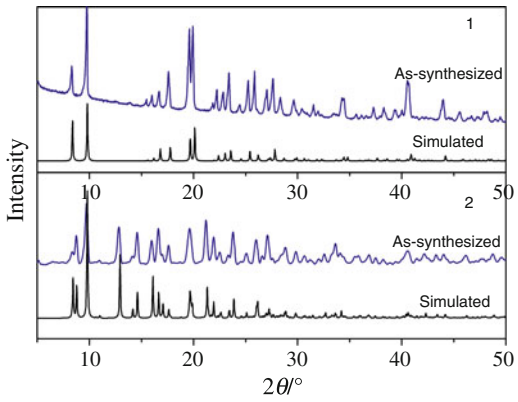

Fig. 1 PXRD patterns of as-synthesized and simulated patterns of **1** and **2**

971 K (**2**). The heating rate was 10 K min^{-1} and the air flow rate was 100 mL min^{-1}. The mass of the compound was about 38.04 mg (**1**) and 43.33 mg (**2**). The TG equipment was calibrated by the $CaC_2O_4{\cdot}H_2O$ (99.9%).

Heat capacity measurement

Heat capacity measurements were performed on DSC Q1000 (T-zero DSC-technology, TA Instruments Inc., USA) with a heating rate of 10 K min^{-1}. Dry high purity nitrogen (99.999%) was used as purge gas at a flow rate of 50 mL min^{-1} through the DSC cell. A mechanical cooling system was used for the experimental measurement. The temperature scale of the instrument was initially calibrated in the standard DSC mode, using the extrapolated onset temperatures of the melting of indium (429.75 K), as described in our previous articles [27–32]. The energy scale was calibrated with the heat of fusion of indium (28.45 J g^{-1}). The heat capacity calibration was made by running a standard sapphire (Al_2O_3) at the experimental temperature. The accuracy of TMDSC is established by comparing the measured heat capacity of standard sapphire with previously reported values [35]. The calibration method and the experiment were performed at the same conditions as follows: (1) sampling interval: 1.00 s/pt; (2) zero heat flow at 428.15 K; (3) equilibrate at 183.15 K; (4) isothermal for 5.00 min; (5) temperature ramp at 10 K min^{-1} to 673.15 K.

The masses of the reference and sample pans with lids were selected to be within 54.53 ± 0.05 mg. Samples were crimped in non-hermetic aluminum pans with lids. Sample mass was weighed on a METTLER TOLEDO electrobalance (AB135-S, Classic) with an accuracy of (±0.01 mg).

Results and discussion

Thermal stabilities and decomposition of **1** and **2**

The TG curve (Fig. 2, right) of **1** shows that the three-stage mass loss occurs in the temperature range of 300 to 1,170 K. The first mass loss starts at about 550 K and is about 22.71%, most probably due to the loss of the DMF molecule (calculated 22.33%). A second loss of 47.20% is observed between 702 and 935 K. It corresponds to the total oxidative degradation of the NDC ligands into CO_2 (acidic character) that instantaneously reacts with the so-generated CaO (base) to yield calcium carbonate (calculated 47.09%). The third stage takes place between 935 and 1,128 K and is accompanied by 13.91% mass loss which is attributed to the loss of CO_2 (calculated 13.44%). The overall mass loss of **1** is 83.82%, in accord with the calculated percentage (82.86%) for CaO as the final residue.

The decomposition of **2** occurs between 300 and 971 K in two steps (Fig. 2, left). A first loss (27.76%), starting at 455 K, is achieved at 667 K and corresponds to the release of all the DMF molecules (calculated 26.59%). From 667 to 840 K, the second loss corresponds to the decomposition of the organic host frameworks. The overall mass loss of **2**, 80.20%, corresponds to Mn_3O_4 as final residue (calculated 79.20%), indicating a partial oxidation of Mn(II) into the more stable mixed oxide.

The above data show that the as-synthesized Ca compound is more stable than its Mn "analog", despite the fact that the ionic radius of Ca(II) (1.14, 1.20, and 1.26 Å for 6-, 7-, and 8-coordinated ion, respectively) is larger than that of Mn(II) (0.81–0.97 Å). This is also confirmed by the crystallographic structure of both MOFs: Ca–O distances: 2.35 Å (6-coordinated Ca), 2.39 Å (7-coordinated Ca),

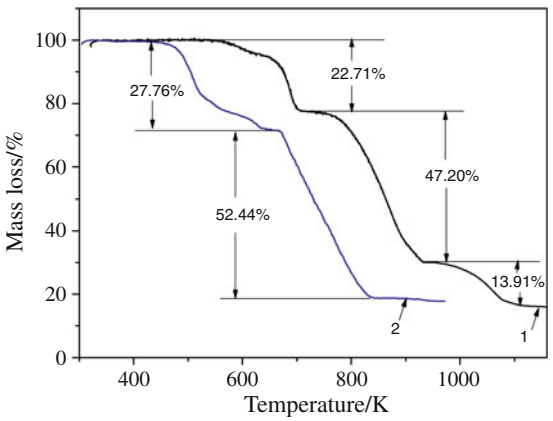

Fig. 2 TG curves of **1** and **2** under air atmosphere at 10 K min^{-1}

2.45 Å (8-coordinated Ca) in **1** and Mn–O distance varying from 1.155 to 1.185 Å in **2**. This apparent discrepancy is easily explained by the fact that the bulky structure is significantly different in both compounds in terms of cationic coordination and clustering (see introduction) but also in terms of porosity. Indeed, the Mn compound forms a 3D network with 1D channels (7 × 7 Å) in which the DMF molecules protrude, being therefore more readily destabilized than in **1**, which has a non porous structure and in which both DMF and the NDC ligands are more tightly retained by Ca^{2+} cations in the bulky structure.

Heat capacity

The heat capacities of **1** and **2** are listed in Tables 1 and 2. The experimental standard deviations are below 0.028 J K^{-1} g^{-1} (for **1**) and 0.022 J K^{-1} g^{-1} (for **2**), resulting in a very good reproducibility of the $C_{p,m}$ values in the experimental temperature range from 198 to 548 K (for **1**) and from 198 to 448 K (for **2**). The experimental molar heat capacities curves of **1** and **2** versus temperature are shown in Fig. 3. The heat capacities of the two samples increase continuously with the increasing temperature, indicating that neither a phase transition nor a thermal anomaly occurs in the experimental temperature range and confirming that both **1** and **2** are stable in the temperature ranges defined for each compound.

The experimental and calculated molar heat capacities data are listed in Table 3 (for **1**) and Table 4 (for **2**). The molar heat capacities are fitted to the following polynomial equation of heat capacities ($C_{p,m}$) with reduced temperature (X), by means of the least square fitting:

T from 198 to 548 K (for **1**)

$$\begin{aligned} C_{p,m,1}\left[\text{J mol}^{-1}\text{K}^{-1}\right] &= 540.1(\pm 0.2735) \\ &+ 187.3(\pm 0.1091)X_1 \\ &- 10.91(\pm 1.667)X_1^2 \\ &- 29.15(\pm 4.175)X_1^3 \\ &- 12.05(\pm 1.813)X_1^4 \\ &+ 33.24(\pm 3.566)X_1^5 \end{aligned} \quad (1)$$

T from 198 to 448 K (for **2**)

$$\begin{aligned} C_{p,m,2}\left[\text{J mol}^{-1}\text{K}^{-1}\right] &= 1544(\pm 0.8257) + 470.1(\pm 3.281)X_2 \\ &+ 4.788(\pm 4.984)X_2^2 \\ &- 85.69(\pm 12.44)X_2^3 \\ &- 9.618(\pm 5.366)X_2^4 \\ &+ 105.8(\pm 10.52)X_2^5 \end{aligned} \quad (2)$$

where $X_1 = (T - 373)/175$, $X_2 = (T - 323)/125$, and T is the experimental temperature, 373 and 323 are obtained from polynomial $(T_{max} + T_{min})/2$, 175 and 125 are

Table 1 The data of three reduplicate experiments for **1** (molecular formula: Ca(2,6-NDC)(DMF), molar mass: 327.35 g mol^{-1})

T/K	$C_{p,m}$ (exp)/J K^{-1} g^{-1}				Standard deviation/ J K^{-1} g^{-1}
	Test 1	Test 2	Test 3	Average	
198	0.9605	1.010	0.9954	0.9886	0.025
203	0.9954	1.045	1.031	1.024	0.026
208	1.019	1.071	1.063	1.051	0.028
213	1.050	1.094	1.089	1.078	0.024
218	1.079	1.113	1.113	1.102	0.019
223	1.107	1.134	1.136	1.126	0.016
228	1.132	1.154	1.157	1.148	0.014
233	1.158	1.174	1.180	1.171	0.011
238	1.180	1.195	1.201	1.192	0.011
243	1.205	1.214	1.223	1.214	0.0090
248	1.228	1.233	1.244	1.235	0.0082
253	1.249	1.250	1.263	1.254	0.0078
258	1.265	1.263	1.277	1.268	0.0076
263	1.279	1.276	1.289	1.281	0.0068
268	1.293	1.288	1.302	1.294	0.0071
273	1.308	1.302	1.317	1.309	0.0075
278	1.324	1.319	1.334	1.326	0.0076
283	1.343	1.337	1.352	1.344	0.0076
288	1.361	1.355	1.370	1.362	0.0076
293	1.382	1.374	1.389	1.382	0.0075
298	1.403	1.392	1.408	1.401	0.0082
303	1.421	1.409	1.426	1.419	0.0087
308	1.440	1.425	1.445	1.437	0.010
313	1.458	1.443	1.464	1.455	0.011
318	1.476	1.459	1.482	1.472	0.012
323	1.494	1.476	1.499	1.490	0.012
328	1.511	1.492	1.517	1.507	0.013
333	1.527	1.508	1.534	1.523	0.013
338	1.545	1.526	1.550	1.540	0.013
343	1.563	1.544	1.567	1.558	0.012
348	1.579	1.561	1.584	1.575	0.012
353	1.593	1.574	1.601	1.589	0.014
358	1.602	1.584	1.609	1.598	0.013
363	1.618	1.598	1.623	1.613	0.013
368	1.637	1.619	1.643	1.633	0.012
373	1.652	1.635	1.659	1.649	0.012
378	1.670	1.653	1.676	1.666	0.012
383	1.684	1.669	1.692	1.682	0.012
388	1.699	1.686	1.706	1.697	0.010
393	1.713	1.701	1.721	1.712	0.010
398	1.729	1.719	1.737	1.728	0.0090
403	1.746	1.736	1.753	1.745	0.0085
408	1.762	1.753	1.768	1.761	0.0076
413	1.776	1.769	1.782	1.776	0.0065
418	1.792	1.786	1.798	1.792	0.0060
423	1.807	1.802	1.812	1.807	0.0050

Table 1 continued

T/K	$C_{p,m}$ (exp)/J K^{-1} g^{-1}				Standard deviation/ J K^{-1} g^{-1}
	Test 1	Test 2	Test 3	Average	
428	1.822	1.821	1.827	1.823	0.0032
433	1.838	1.840	1.844	1.840	0.0030
438	1.850	1.856	1.856	1.854	0.0035
443	1.864	1.871	1.87	1.868	0.0038
448	1.875	1.887	1.882	1.881	0.0060
453	1.888	1.903	1.895	1.895	0.0075
458	1.901	1.920	1.910	1.910	0.0095
463	1.915	1.931	1.923	1.923	0.0080
468	1.927	1.952	1.937	1.939	0.013
473	1.939	1.966	1.951	1.952	0.014
478	1.954	1.980	1.964	1.966	0.013
483	1.966	1.995	1.978	1.980	0.015
488	1.980	2.006	1.992	1.993	0.013
493	1.995	2.019	2.008	2.007	0.012
498	2.007	2.030	2.019	2.018	0.012
503	2.021	2.045	2.033	2.033	0.012
508	2.035	2.058	2.046	2.046	0.011
513	2.047	2.068	2.062	2.059	0.011
518	2.061	2.083	2.076	2.073	0.011
523	2.075	2.095	2.09	2.087	0.010
528	2.088	2.108	2.105	2.100	0.011
533	2.105	2.120	2.120	2.115	0.0087
538	2.118	2.135	2.136	2.130	0.010
543	2.138	2.154	2.152	2.148	0.0088
548	2.154	2.173	2.17	2.166	0.010

obtained from polynomial $(T_{max} - T_{min})/2$, where T_{max} is the upper limit of the above temperature region, and T_{min} is the lower limit of the above temperature region. The correlation coefficients of the fitting are: $R_1^2 = 0.9999$ and $R_2^2 = 0.9999$. The relative deviations of all the experimental points from the fitting heat capacity values are within ±0.75% (for **1**) in Table 3 and ±0.54% (for **2**) in Table 4. Relative deviations have been calculated by the following equation:

$$RD(\%) = 100\left[C_{p,m}(\text{exp}) - C_{p,m}(\text{fit})\right]/C_{p,m}(\text{fit}) \quad (3)$$

where $C_{p,m}$(exp) is the experimental molar heat capacity and $C_{p,m}$(fit) is the calculated heat capacity. Based on Eq. 1, the heat capacity of **1** at 298.15 K was calculated to be 549.4 J mol^{-1} K^{-1}, and based on Eq. 2, the heat capacity of **2** at 298.15 K was calculated to be 1,541 J mol^{-1} K^{-1}.

Thermodynamic functions

Enthalpy and entropy of substances are basic thermodynamic functions. Through the polynomial representing heat

Table 2 The data of three reduplicate experiments for **2** (molecular formula: $Mn_3(2,6\text{-NDC})_3(DMF)_4$, molar mass: 1099.71 g mol^{-1})

T/K	$C_{p,m}$(exp)/J K^{-1} g^{-1}				Standard deviation/ J K^{-1} g^{-1}
	Test 1	Test 2	Test 3	Average	
198	0.9517	0.9607	0.9337	0.9490	0.014
203	0.987	0.9993	0.9667	0.9840	0.016
208	1.009	1.022	0.9884	1.006	0.017
213	1.030	1.046	1.010	1.029	0.018
218	1.051	1.068	1.029	1.049	0.020
223	1.07	1.089	1.049	1.069	0.020
228	1.088	1.108	1.067	1.088	0.021
233	1.107	1.126	1.085	1.106	0.021
238	1.125	1.146	1.104	1.125	0.021
243	1.143	1.164	1.122	1.143	0.021
248	1.162	1.182	1.14	1.161	0.021
253	1.177	1.198	1.156	1.177	0.021
258	1.191	1.211	1.169	1.190	0.021
263	1.204	1.224	1.182	1.203	0.021
268	1.217	1.237	1.196	1.217	0.020
273	1.232	1.252	1.21	1.231	0.021
278	1.247	1.268	1.226	1.247	0.021
283	1.265	1.285	1.243	1.264	0.021
288	1.283	1.305	1.263	1.284	0.021
293	1.304	1.325	1.283	1.304	0.021
298	1.321	1.343	1.300	1.321	0.022
303	1.339	1.359	1.318	1.339	0.020
308	1.355	1.377	1.336	1.356	0.021
313	1.372	1.393	1.353	1.373	0.020
318	1.390	1.410	1.371	1.390	0.019
323	1.405	1.426	1.388	1.406	0.019
328	1.424	1.443	1.406	1.424	0.018
333	1.439	1.458	1.422	1.440	0.018
338	1.455	1.475	1.440	1.457	0.017
343	1.472	1.492	1.457	1.474	0.018
348	1.489	1.508	1.473	1.490	0.017
353	1.503	1.523	1.488	1.505	0.017
358	1.515	1.535	1.501	1.517	0.017
363	1.532	1.552	1.519	1.534	0.016
368	1.552	1.570	1.537	1.553	0.016
373	1.567	1.588	1.555	1.570	0.016
378	1.583	1.605	1.572	1.587	0.017
383	1.601	1.621	1.589	1.604	0.016
388	1.614	1.636	1.604	1.618	0.016
393	1.631	1.654	1.621	1.635	0.017
398	1.647	1.670	1.637	1.651	0.017
403	1.664	1.687	1.654	1.668	0.017
408	1.681	1.704	1.67	1.685	0.017
413	1.697	1.721	1.687	1.702	0.017
418	1.715	1.739	1.706	1.720	0.017
423	1.733	1.756	1.723	1.737	0.019

Table 2 continued

T/K	$C_{p,m}$(exp)/J K^{-1} g^{-1}				Standard deviation/ J K^{-1} g^{-1}
	Test 1	Test 2	Test 3	Average	
428	1.752	1.776	1.743	1.757	0.017
433	1.774	1.796	1.763	1.778	0.016
438	1.794	1.818	1.784	1.799	0.017
443	1.815	1.839	1.806	1.820	0.017
448	1.838	1.862	1.827	1.842	0.018

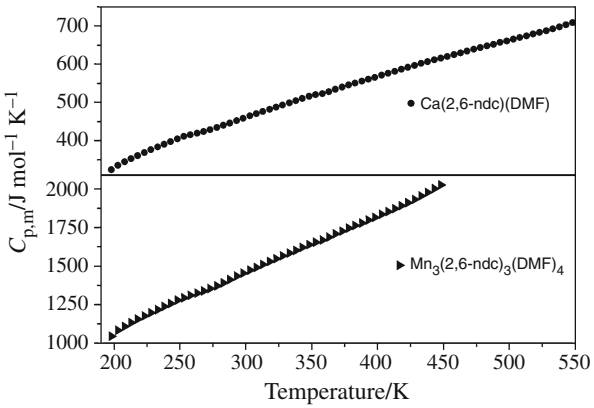

Fig. 3 Molar heat capacities ($C_{p,m}$) of **1** and **2** as a function of temperature

capacity and the relationship between thermodynamic functions and heat capacity, the thermodynamic functions relative to the reference temperature of 298.15 K were calculated from 198 to 548 K (for **1**) and from 198 to 448 K (for **2**) with an interval of 5 K. The thermodynamic relationships are as follows:

$$H_T - H_{298.15} = \int_{298.15}^{T} C_{p,m}\mathrm{d}T \quad (4)$$

$$S_T - S_{298.15} = \int_{298.15}^{T} (C_{p,m}/T)\mathrm{d}T \quad (5)$$

The calculated thermodynamic functions $[H_T - H_{298.15}]$ and $[S_T - S_{298.15}]$ are listed in Table 5 (for **1**) and in Table 6 (for **2**). It can be seen that both functions $[H_T - H_{298.15}]$ and $[S_T - S_{298.15}]$ of **1** and **2** increase with increasing temperature in a continuous way, within the given temperature range.

Besides the fundamental and practical importance in compiling various thermodynamic parameters (here $C_{p,m}$, ΔH and ΔS) and their variation with temperature for the two compounds investigated in this study, we have compared the present values with those obtained by our group using the same experimental methods for three other MOF-type materials based on NDC and optionally DMF in their structure, namely Li_2(2,6-NDC) [24], Li_2(1,4-NDC)(DMF) [26], and Mg(2,6-NDC)$(DMF)_{0.66}$ [31]. While the $C_{p,m}$, ΔH and ΔS values are relatively close for the above studied Ca and Mn compounds, the same parameters for the other three samples give markedly different and random values, confirming that their thermodynamic parameters are rather related to the structure of the compounds than to the nature of their constituents.

Table 3 The experimental and calculated molar heat capacities of **1**

T/ K	$C_{p,m}$ (exp)/ J K^{-1} mol^{-1}	$C_{p,m}$ (fit)/ J K^{-1} mol^{-1}	T/ K	$C_{p,m}$ (exp)/ J K^{-1} mol^{-1}	$C_{p,m}$ (fit)/ J K^{-1} mol^{-1}
198	323.6	325.8	378	545.5	545.4
203	335.1	335.1	383	550.5	550.8
208	344.0	343.9	388	555.5	556.1
213	352.8	352.4	393	560.3	561.3
218	360.6	360.4	398	565.8	566.5
223	368.5	368.0	403	571.2	571.7
228	375.7	375.3	408	576.5	576.9
233	383.2	382.4	413	581.3	582.0
238	390.2	389.2	418	586.6	587.0
243	397.4	395.7	423	591.5	592.0
248	404.3	402.1	428	596.9	597.0
253	410.5	408.2	433	602.5	601.9
258	415.2	414.3	438	606.9	606.7
263	419.4	420.2	443	611.6	611.4
268	423.7	425.9	448	615.9	616.1
273	428.5	431.6	453	620.4	620.8
278	434.0	437.3	458	625.3	625.4
283	440.0	442.8	463	629.5	629.9
288	445.9	448.3	468	634.6	634.4
293	452.3	453.8	473	639.0	638.9
298	458.6	459.2	478	643.6	643.3
303	464.4	464.7	483	648.0	647.7
308	470.3	470.1	488	652.3	652.0
313	476.3	475.5	493	657.1	656.4
318	482.0	480.8	498	660.8	660.7
323	487.6	486.2	503	665.5	665.1
328	493.2	491.6	508	669.9	669.5
333	498.6	497.0	513	674.0	674.0
338	504.2	502.4	518	678.7	678.5
343	510.0	507.8	523	683.1	683.1
348	515.5	513.2	528	687.5	687.9
353	520.3	518.6	533	692.3	692.8
358	523.2	524.0	538	697.1	697.8
363	528.0	529.4	543	703.1	703.1
368	534.6	534.7	548	708.9	708.5
373	539.7	540.1			

Table 4 The experimental and calculated molar heat capacities of **2**

T/K	$C_{p,m}$ (exp)/ J K^{-1} mol^{-1}	$C_{p,m}$ (fit)/ J K^{-1} mol^{-1}	T/K	$C_{p,m}$ (exp)/ J K^{-1} mol^{-1}	$C_{p,m}$ (fit)/ J K^{-1} mol^{-1}
198	1,043	1,049	328	1,566	1,563
203	1,082	1,078	333	1,583	1,582
208	1,107	1,106	338	1,602	1,600
213	1,131	1,131	343	1,621	1,619
218	1,154	1,154	348	1,639	1,638
223	1,176	1,176	353	1,655	1,656
228	1,196	1,197	358	1,668	1,674
233	1,216	1,217	363	1,687	1,692
238	1,237	1,236	368	1,708	1,710
243	1,257	1,255	373	1,727	1,728
248	1,277	1,273	378	1,745	1,746
253	1,294	1,291	383	1,764	1,763
258	1,309	1,308	388	1,779	1,781
263	1,323	1,326	393	1,798	1,799
268	1,338	1,343	398	1,816	1,816
273	1,354	1,361	403	1,835	1,834
278	1,371	1,379	408	1,853	1,852
283	1,390	1,396	413	1,871	1,871
288	1,412	1,414	418	1,892	1,890
293	1,434	1,433	423	1,911	1,910
298	1,453	1,451	428	1,932	1,931
303	1,472	1,469	433	1,955	1,953
308	1,491	1,488	438	1,978	1,977
313	1,510	1,506	443	2,001	2,002
318	1,529	1,525	448	2,026	2,029
323	1,547	1,544			

Table 5 Calculated thermodynamic function data of **1**

T/K	$H_T - H_{298.15}$/ kJ mol^{-1}	$S_T - S_{298.15}$/ J K^{-1} mol^{-1}	T/K	$H_T - H_{298.15}$/ kJ mol^{-1}	$S_T - S_{298.15}$/ J K^{-1} mol^{-1}
198	−39.97	−161.6	373	37.41	111.6
203	−38.31	−153.3	378	40.12	118.8
208	−36.61	−145.0	383	42.86	126.0
213	−34.88	−136.7	388	45.63	133.2
218	−33.09	−128.4	393	48.42	140.3
223	−31.27	−120.2	398	51.24	147.4
228	−29.41	−111.9	403	54.09	154.5
233	−27.52	−103.7	408	56.96	161.6
238	−25.59	−95.55	413	59.86	168.6
243	−23.63	−87.40	418	62.78	175.7
248	−21.63	−79.28	423	65.72	182.7
253	−19.61	−71.20	428	68.70	189.7
258	−17.55	−63.15	433	71.70	196.7
263	−15.47	−55.15	438	74.72	203.6
268	−13.35	−47.18	443	77.76	210.5
273	−11.20	−39.26	448	80.83	217.4
278	−9.035	−31.37	453	83.93	224.3
283	−6.835	−23.53	458	87.04	231.1

Table 5 continued

T/K	$H_T - H_{298.15}$/ kJ mol^{-1}	$S_T - S_{298.15}$/ J K^{-1} mol^{-1}	T/K	$H_T - H_{298.15}$/ kJ mol^{-1}	$S_T - S_{298.15}$/ J K^{-1} mol^{-1}
288	−4.607	−15.72	463	90.18	238.0
293	−2.351	−7.958	468	93.34	244.8
298	−0.06890	−0.2312	473	96.52	251.5
298.15	0	0	478	99.73	258.3
303	2.241	7.457	483	102.9	264.9
308	4.578	15.11	488	106.2	271.7
313	6.941	22.72	493	109.5	278.3
318	9.332	30.30	498	112.7	285.0
323	11.75	37.84	503	116.1	291.6
328	14.19	45.35	508	119.4	298.2
333	16.66	52.83	513	122.8	304.8
338	19.16	60.27	518	126.2	311.3
343	21.69	67.69	523	129.5	317.8
348	24.24	75.07	528	132.9	324.4
353	26.82	82.42	533	136.4	330.8
358	29.43	89.75	538	139.9	337.4
363	32.06	97.05	543	143.4	343.8
368	34.72	104.3	548	146.9	350.3

Table 6 Calculated thermodynamic function data of **2**

T/K	$H_T - H_{298.15}$/ kJ mol^{-1}	$S_T - S_{298.15}$/ J K^{-1} mol^{-1}	T/K	$H_T - H_{298.15}$/ kJ mol^{-1}	$S_T - S_{298.15}$/ J K^{-1} mol^{-1}
198	−126.8	−513.2	323	37.21	119.8
203	−121.5	−486.5	328	44.98	143.6
208	−116.1	−459.8	333	52.84	167.4
213	−110.5	−433.2	338	60.80	191.1
218	−104.7	−406.7	343	68.84	214.8
223	−98.90	−380.3	348	76.99	238.3
228	−93.00	−354.0	353	85.22	261.8
233	−86.96	−327.9	358	93.54	285.2
238	−80.82	−301.9	363	101.9	308.6
243	−74.60	−276.0	368	110.4	331.8
248	−68.28	−250.3	373	119.1	355.1
253	−61.87	−224.7	378	127.7	378.2
258	−55.37	−199.3	383	136.5	401.2
263	−48.79	−174.0	388	145.4	424.2
268	−42.12	−148.8	393	154.3	447.2
273	−35.36	−123.8	398	163.4	470.0
278	−28.51	−98.98	403	172.5	492.8
283	−21.57	−74.24	408	181.7	515.5
288	−14.54	−49.62	413	191.0	538.2
293	−7.426	−25.12	418	200.4	560.8
298	−0.2177	−0.7302	423	209.9	583.4
298.15	0	0	428	219.5	605.9
303	7.082	23.56	433	229.2	628.4
308	14.47	47.75	438	239.0	651.0
313	21.96	71.85	443	249.0	673.6
318	29.54	95.87	448	259.1	696.2

Conclusions

Two microporous metal-organic frameworks, Ca(2,6-NDC)(DMF) (**1**) and Mn_3(2,6-NDC)$_3$(DMF)$_4$ (**2**), of similar composition but structurally unrelated, have been solvothermally synthesized and characterized. In particular, the TG curves of the two compounds had shown that they are thermally stable in the temperature range 300–550 K (for **1**) and 300 to 455 K (for **2**), thereby defining the temperature domains under which various thermodynamic properties can be determined. The molar heat capacities were measured from 198 to 548 K (for **1**) and from 198 to 448 K (for **2**) by TMDSC for the first time. The heat capacities at 298.15 K were calculated to be 549.4 J mol^{-1} K^{-1} (for **1**) and 1,541 J mol^{-1} K^{-1} (for **2**). The thermodynamic function data (enthalpy and entropy) relative to the reference temperature (298.15 K) were calculated with a temperature interval of 5 K.

Acknowledgements The authors gratefully acknowledge the financial support for this work from the National Natural Science Foundation of China (No. 20833009, 51071146, 51071081, 20873148, 20903095, 50901070 and U0734005), the National Basic Research Program (973 program) of China (2010CB631303), IUPAC (Project No. 2008-006-3-100), Dalian Science and Technology Foundation (2009A11GX052) and the State Key Laboratory of Explosion Science and Technology, Beijing Institute of Technology (Grant No. KFJJ10-1Z).

References

1. Botas JA, Calleja G, Sanchez-Sanchez M, Orcajo MG. Cobalt doping of the MOF-5 framework and its effect on gas-adsorption properties. Langmuir. 2010;26:5300–3.
2. Saha D, Bao ZB, Jia F, Deng SG. Adsorption of CO_2, CH_4, N_2O, and N_2 on MOF-5, MOF-177, and Zeolite 5A. Environ Sci Technol. 2010;44:1820–6.
3. Wang CY, Tsao CS, Yu MS, Liao PY, Chung TY, Wu HC, Miller MA, Tzeng YR. Hydrogen storage measurement, synthesis and characterization of metal-organic frameworks via bridged spillover. J Alloy Compd. 2010;492:88–94.
4. Wang ZQ, Tanabe KK, Cohen SM. Tuning hydrogen sorption properties of metal-organic frameworks by postsynthetic covalent modification. Chem-Eur J. 2010;16:212–7.
5. Zou XL, Cha MH, Kim S, Nguyen MC, Zhou G, Duan WH, Ihm J. Hydrogen storage in Ca-decorated, B-substituted metal organic framework. Int J Hydrog Energy. 2010;35:198–203.
6. Li JR, Kuppler RJ, Zhou HC. Selective gas adsorption and separation in metal-organic frameworks. Chem Soc Rev. 2009;38:1477–504.
7. Liang ZJ, Marshall M, Chaffee AL. CO_2 adsorption-based separation by metal organic framework (Cu-BTC) versus zeolite (13×). Energ Fuel. 2009;23:2785–9.
8. Tagliabue M, Farrusseng D, Valencia S, Aguado S, Ravon U, Rizzo C, Corma A, Mirodatos C. Natural gas treating by selective adsorption: material science and chemical engineering interplay. Chem Eng J. 2009;155:553–66.
9. Gu ZY, Jiang DQ, Wang HF, Cui XY, Yan XP. Adsorption and separation of xylene isomers and ethylbenzene on two Zn-terephthalate metal-organic frameworks. J Phys Chem C. 2010;114:311–6.
10. Xu Q, Liu DH, Yang QY, Zhong CL, Mi JG. Li-modified metal-organic frameworks for CO_2/CH_4 separation: a route to achieving high adsorption selectivity. J Mater Chem. 2010;20:706–14.
11. Song JL, Zhang ZF, Hu SQ, Wu TB, Jiang T, Han BX. MOF-5/*n*-Bu_4NBr: an efficient catalyst system for the synthesis of cyclic carbonates from epoxides and CO_2 under mild conditions. Green Chem. 2009;11:1031–6.
12. Vitorino MJ, Devic T, Tromp M, Ferey G, Visseaux M. Lanthanide metal-organic frameworks as ziegler-natta catalysts for the selective polymerization of isoprene. Macromol Chem Phys. 2009;210:1923–32.
13. Bhattacharjee S, Choi JS, Yang ST, Choi SB, Kim J, Ahn WS. Solvothermal synthesis of Fe-MOF-74 and its catalytic properties in phenol hydroxylation. J Nanosci Nanotechnol. 2010;10:135–41.
14. Juan-Alcaniz J, Ramos-Fernandez EV, Lafont U, Gascon J, Kapteijn F. Building MOF bottles around phosphotungstic acid ships: one-pot synthesis of bi-functional polyoxometalate-MIL-101 catalysts. J Catal. 2010;269:229–41.
15. Kleist W, Maciejewski M, Baiker A. MOF-5 based mixed-linker metal-organic frameworks: synthesis, thermal stability and catalytic application. Thermochim Acta. 2010;499:71–8.
16. Wang MS, Guo SP, Li Y, Cai LZ, Zou JP, Xu G, Zhou WW, Zheng FK, Guo GC. A direct white-light-emitting metal-organic framework with tunable yellow-to-white photoluminescence by variation of excitation light. J Am Chem Soc. 2009;131:13572–3.
17. Wen LL, Wang D, Wang CG, Wang F, Li DF, Deng KJ. A 3D porous zinc MOF constructed from a flexible tripodal ligand: synthesis, structure, and photoluminescence property. J Solid State Chem. 2009;182:574–9.
18. Zhang KL, Pan ZC, Chang Y, Liu WL, Ng SW. Synthesis and characterization of an energetic three-dimensional metal-organic framework with blue photoluminescence. Mater Lett. 2009; 63:2136–8.
19. Loiseau T, Mellot-Draznieks C, Muguerra H, Ferey G, Haouas M, Taulelle F, Chim CR. Hydrothermal synthesis and crystal structure of a new three-dimensional aluminum-organic framework MIL-69 with 2,6-naphthalenedicarboxylate (ndc), Al(OH)(ndc)center dot H_2O. 2005; 8:765–72.
20. Irena S, Julia F, Stefan K. New polymorphs of magnesium-based metal-organic frameworks Mg_3(ndc)$_3$(ndc = 2,6-Naphthalenedicarboxylate). Eur J Inorg Chem. 2007;35:5475–9.
21. Eddaoudi M, Kim J, Rosi N, Vodak D, Wachter J, O'Keeffe M, Yaghi OM. Systematic design of pore size and functionality in isoreticular MOFs and their application in methane storage. Science. 2002;295:469–72.
22. Dinca M, Long JR. Strong H_2 binding and selective gas adsorption within the microporous coordination solid $Mg_3(O_2C–C_{10}H_6–CO_2)_3$. J Am Chem Soc. 2005;127:9376–7.
23. Dailly A, Vajo JJ, Ahn CC. Saturation of hydrogen sorption in Zn benzenedicarboxylate and Zn naphthalenedicarboxylate. J Phys Chem B. 2006;110:1099–101.
24. Jiang CH, Song LF, Jiao CL, Zhang J, Sun LX, Xu F. Exceptional thermal stability and thermodynamic properties of lithium based metal-organic framework. J Therm Anal Calorim. doi: 10.1007/s10973-010-0880-z.
25. Rowsell JLC, Yaghi OM. Strategies for hydrogen storage in metal-organic frameworks. Angew Chem Int Ed. 2005;44:4670–9.
26. Liu YY, Zhang J, Xu F, Sun LX, Zhang T, You WS, Zhao Y, Zeng JL, Cao Z, Yang DW. Lithium-based 3D coordination polymer with hydrophilic structure for sensing of solvent molecules. Cryst Growth Des. 2008;8:3127–9.
27. Qiu SJ, Chu HL, Zhang J, Qi YN, Sun LX, Xu F. Heat capacities and thermodynamic properties of CoPc and CoTMPP. J Therm Anal Calorim. 2008;91:841–8.

28. Qi YN, Xu F, Ma HJ, Sun LX, Zhang J, Jiang T. Thermal stability and glass transition behavior of PANI/gamma-Al_2O_3 composites. J Therm Anal Calorim. 2008;91:219–23.
29. Song LF, Jiang CH, Jiao CL, Zhang J, Sun LX, Xu F, Jiao QZ, Xing YH, Du Y, Cao Z. Heat capacities and thermodynamic properties of one manganese based MOFs. J Therm Anal Calorim. doi:10.1007/s10973-010-0808-7.
30. Zhang J, Zeng JL, Liu YY, Sun LX, Xu F, You WS, Sawada Y. Thermal decomposition kinetics of the synthetic complex Pb(1,4-BDC)center dot(DMF)(H_2O). J Therm Anal Calorim. 2008;91:189–93.
31. Song LF, Jiao CL, Jiang CH, Zhang J, Sun LX, Xu F, Jiao QZ, Xing YH, Huang FL, Du Y. Heat capacities and thermodynamic properties of MgNDC. J Therm Anal Calorim. doi:10.1007/s10973-010-0777-x.
32. Jiang CH, Song LF, Zhang J, Sun LX, Xu F, Li F. Thermodynamic properties and heat capacities of Co (BTC) 1/3 (DMF) (HCOO). J Therm Anal Calorim. 2010. doi:10.1007/s10973-010-0777-x.
33. Williams GA, Blake AJ, Wilson C, Hubberstey P, Schröder M. Novel metal-organic frameworks derived from group II metal cations and aryldicarboxylate anionic ligands. Cryst Growth Des. 2008;8:911–22.
34. Liu B, Zou RQ, Zhong RQ, Han S, Yamada HS, Maruta G, Takeda S, Xu Q. Microporous coordination polymers of cobalt(II) and manganese(II) 2,6-naphthalenedicarboxylate: preparations, structures and gas sorptive and magnetic properties. Microporous Mesoporous Mater. 2008;11:470–7.
35. Archer DG. Thermodynamic properties of synthetic sapphire (alpha-Al_2O_3), standard reference material 720 and the effect of temperature-scale differences on thermodynamic properties. J Phys Chem Ref Data. 1993;22:1441–53.